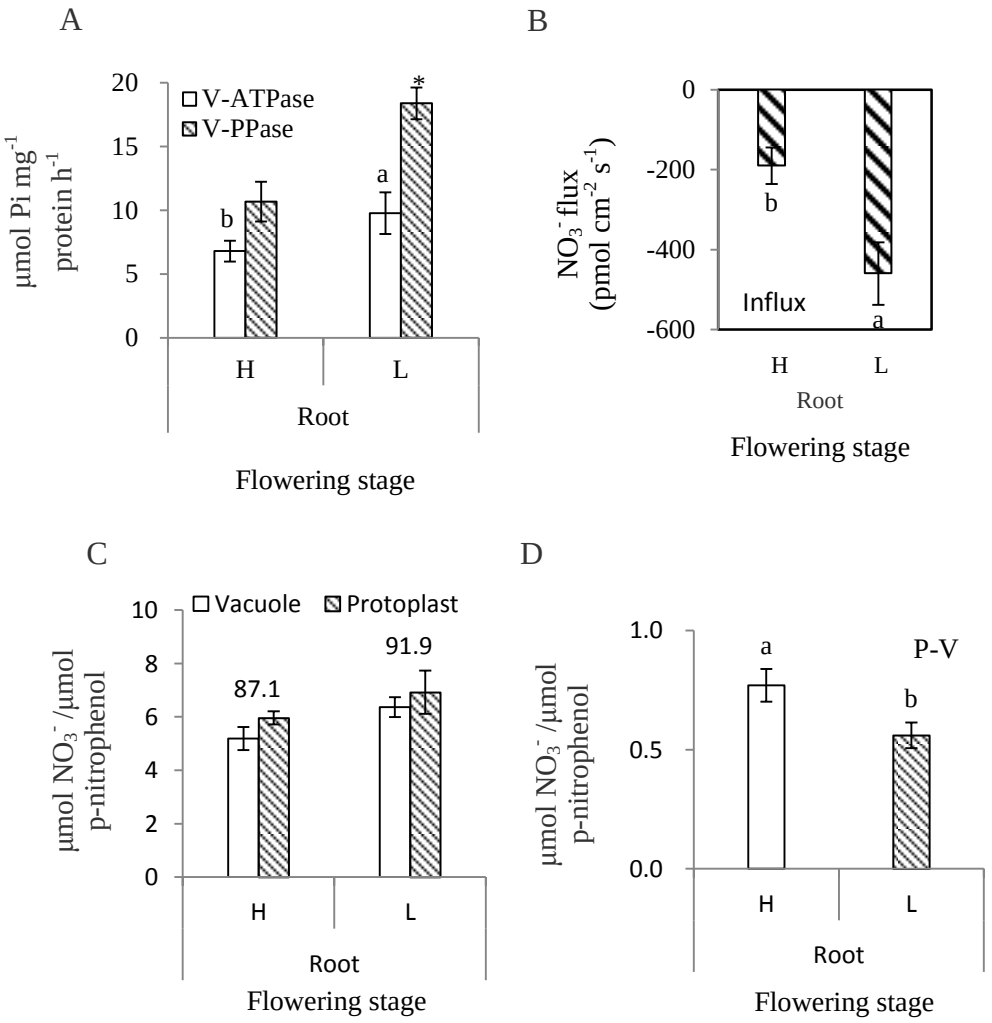

Supplemental Figure 1. *B. napus* with higher NUE showed lower vacuolar sequestration capacity (VSC) for NO_3^- in roots at flowering stage.

H refers to the high-NUE oilseed rape genotype Xiangyou15 and L refers to the low-NUE genotype 814. Specific activities of the tonoplast proton pumps are expressed as μmol Pi released mg^{-1} protein h^{-1}. NO_3^- fluxes are expressed as pmol NO_3^- cm^2 S^{-1}. Mature vacuoles were collected from root tissues at the flowering stage. A microelectrode was vibrated in the measuring solution between the two positions, 1 μm and 11 μm from the vacuole surface (tonoplast), along an axis perpendicular to the tangent of vacuoles recording the stable reading data. The background was recorded by vibrating the electrode in measuring solution without vacuoles. Protoplasts and vacuoles isolated from roots of hydroponically grown plants were used for measuring NO_3^- concentration and NO_3^- accumulation normalized against the specific activity of the vacuole acid phosphatase (ACP) as described in Materials and Methods; thus plotted as μmol NO_3^- per μmol *p*-nitrophenol, the end product of ACP assay.

Proton pump activities in root tissues of H and L genotypes are shown at flowering stage **(A)**. Different letters at the top of the histogram bars denote significant differences in V-ATPase activity in root tissues of H and L genotypes (P<0.05); an asterisk (*) at the top of the histogram bars denote significant differences between V-PPase in root tissues of H and L genotypes (P<0.05). Vertical bars indicate SD (n=6).

Mean rates of NO_3^- flux during 160 s within vacuoles of root tissues of H and L genotypes at flowering stage **(B)**. Different letters at the top of the histogram bars denote significant differences in NO_3^- flux between H and L genotypes (P<0.05). Vertical bars indicate SD (n=6).

Accumulation of NO_3^- in the vacuole and in the protoplasts of root tissues at the flowering stage **(C)**. Values above the bars represent the percentage of vacuolar NO_3^- relative to the total NO_3^- in protoplasts.

NO_3^- accumulation in the cytosol of root tissues at flowering **(D)**. P-V is the total NO_3^- in the cytosol and was calculated as total NO_3^- in protoplasts – total NO_3^- in vacuole. Different letters at the top of the histogram bars denote significant differences in total NO_3^- between H and L genotypes (P<0.05). Vertical bars indicate SD (n=6).

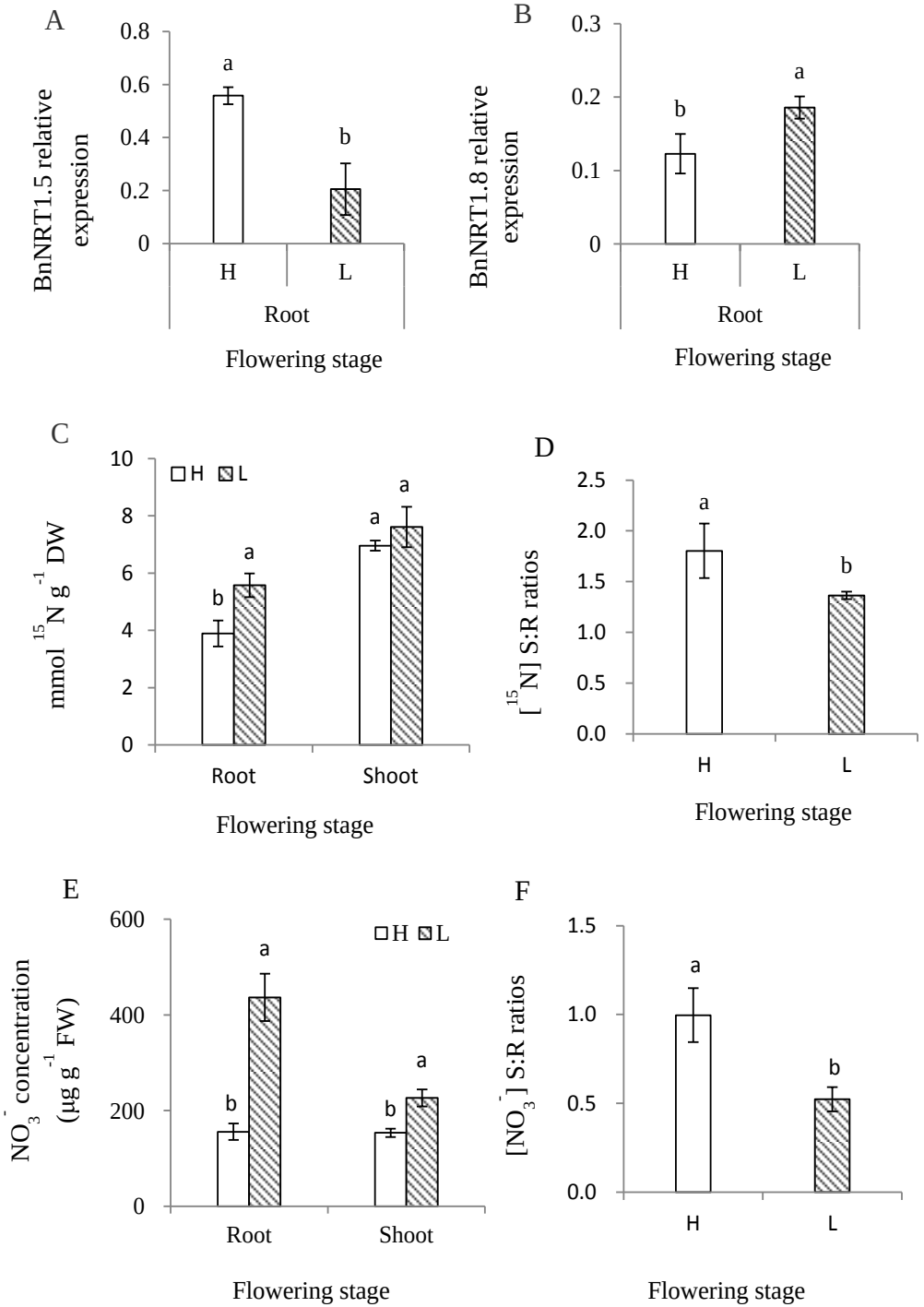

Supplemental Figure 2. *B. napus* with higher NUE showed enhanced long-distance transport of NO_3^- from roots to shoots at flowering stage.

H refers to the high-NUE genotype Xiangyou15 and L refers to the low-NUE genotype 814.

Expression of *BnNRT1.5* (**A**) and *BnNRT1.8* (**B**) genes relative to that of the actin gene in root tissues of the two genotypes at flowering stage assessed by quantitative RT-PCR as described in Materials and Methods; a value of 1.0 is equivalent to the level of expression of the *Bnactin* gene. Vertical bars indicate SD (n=3); different letters at the top of the histogram bars denote significant differences at $P<0.05$.

Hydroponically grown *B. napus* plants were subjected to ^{15}N-labeling treatment as described in Materials and Methods. The ^{15}N content in root and shoot tissues of the two genotypes is shown at flowering stage **(C)**. The [^{15}N]S:R ratios in root and shoot tissues of the two genotypes at flowering stage **(D)**.Vertical bars indicate SD (n=3), different letters at the top of the histogram bars denote significant differences at $P<0.05$.

The NO_3^- concentration (μg g^{-1} FW) in root and shoot tissues of the two genotypes are shown at the flowering stage **(E)**. The [NO_3^-]S:R ratios of the two genotypes at the flowering **(F)**.Vertical bars indicate SD (n=3), different letters at the top of the histogram bars denote significant differences at $P<0.05$ level.

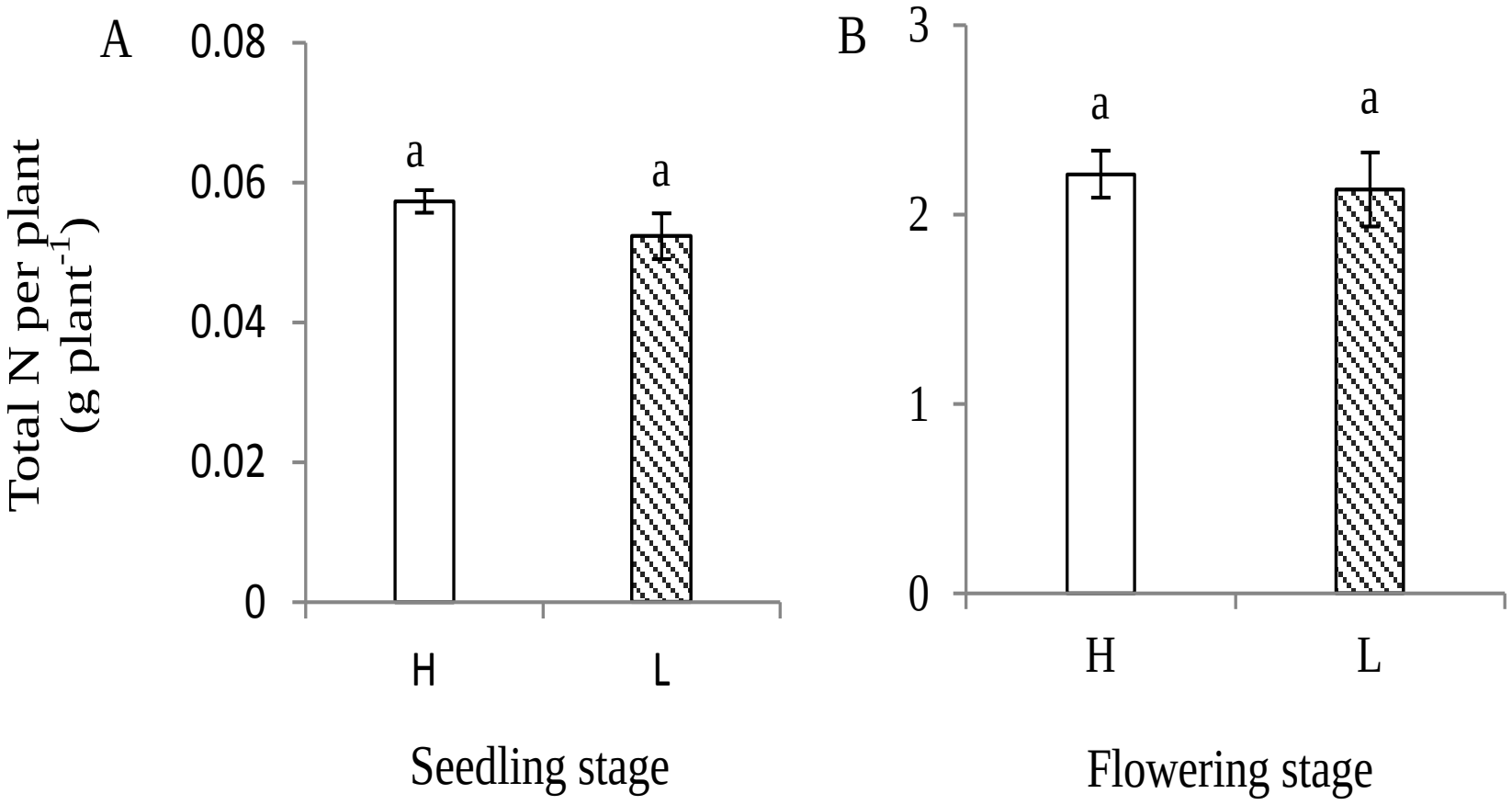

Supplemental Figure 3. The two *B. napus* (H and L genotypes) showed the same total N per plant at seedling stage (**A**) and flowering stage (**B**).
B. napus H and L genotypes are described in Materials and Methods. Vertical bars indicate SD (n=3), different letters at the top of the histogram bars denote significant differences at $P<0.05$.

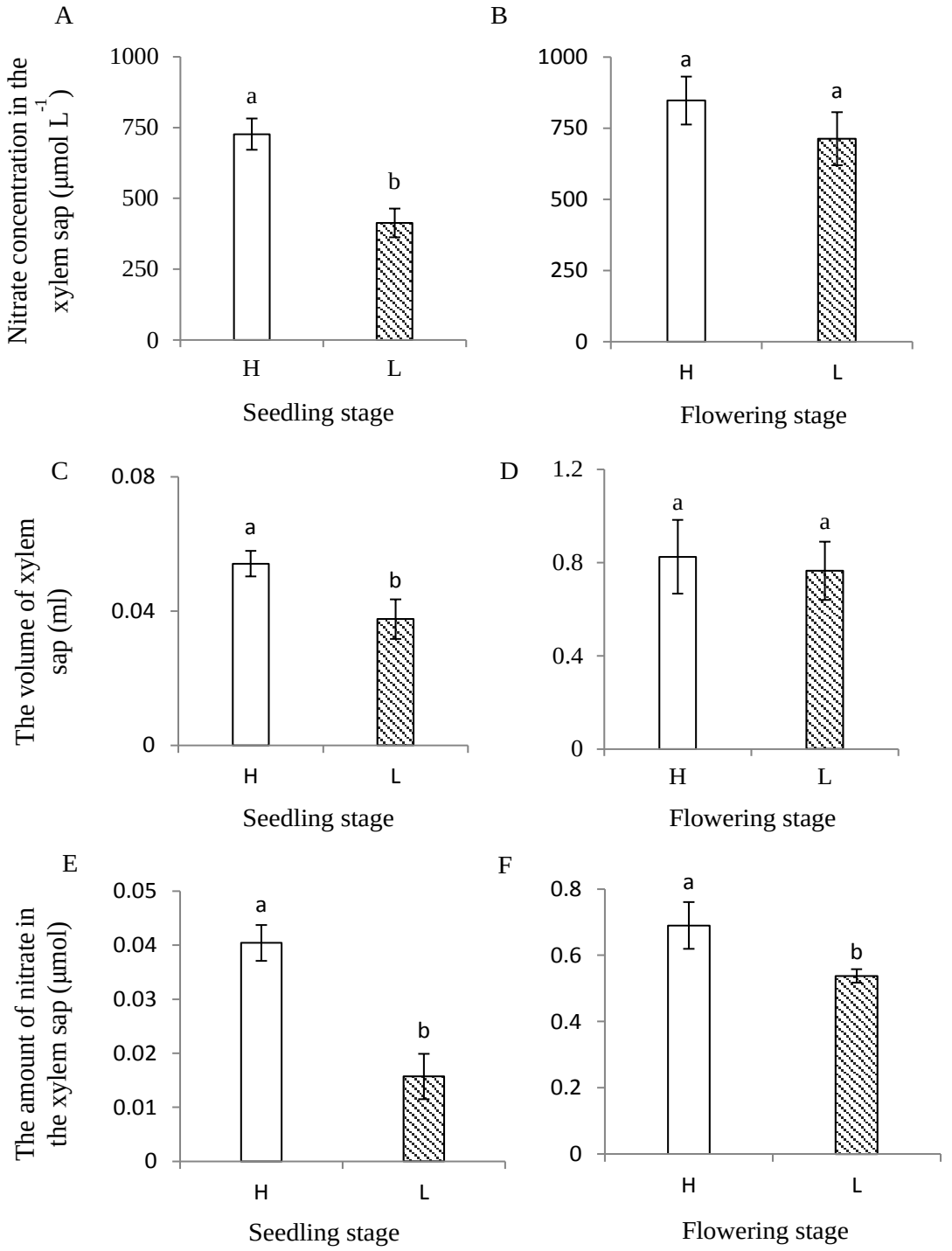

Supplemental Figure 4. *B. napus* with higher NUE showed increased NO_3^- concentration in the xylem sap at seedling and flowering stages. *B. napus* genotypes H and L are described in Materials and Methods. NO_3^- concentrations in the xylem sap of the two genotypes are shown at seedling **(A)** and at flowering **(B)** stages, respectively. Volume of xylem sap collected in 1h from the two genotypes is shown at seedling stage **(C)** and at flowering stage **(D)**. Amount of NO_3^- in the xylem sap from the two genotypes at seedling stage **(E)** and flowering stage**(F)**. Vertical bars indicate SD (n=3), different letters at the top of the histogram bars denote significant differences at $P<0.05$ level.

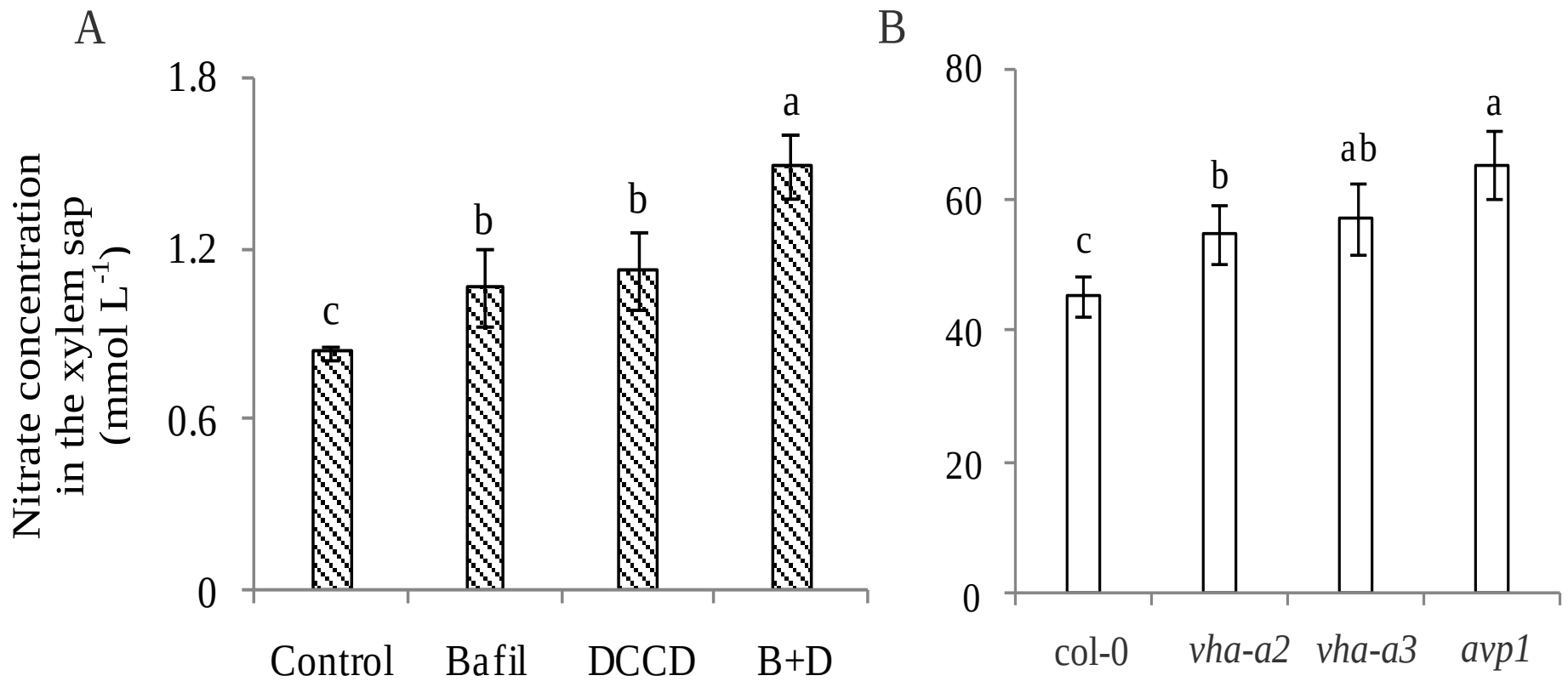

Supplemental Figure 5. NO_3^- concentration in the xylem sap as affected by inhibitor treatments in *B. napus* and in the energy pumps' mutants of *A. thaliana* (col-0, *vha-a2, vha-a3, avp1*). Inhibitors were applied in the hydroponic solution. *A. thaliana* plants were as defined in the legend to Fig. 4. Growth conditions for hydroponically grown plants with ^{15}N treatment are described in Materials and Methods. NO_3^- concentration in the xylem sap as affected by inhibitor treatments are depicted for *B. napus* **(A)** and for various *A. thaliana* **(B)**. Different letters at the top of the histogram bars denote significant differences ($P<0.05$). Vertical bars on the figures indicate SD (n=3).

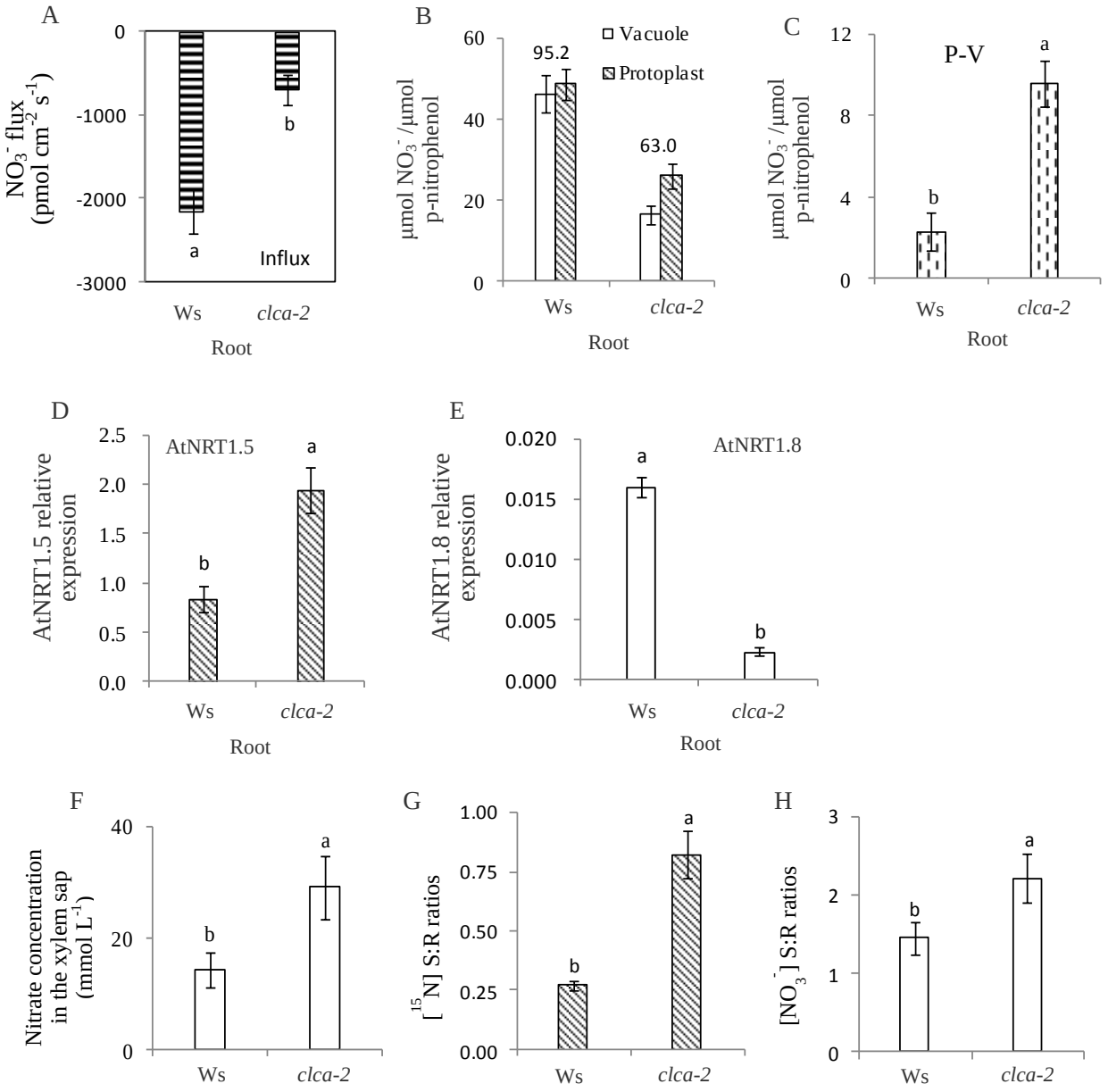

Supplemental Figure 6. Reduced VSC for NO_3^- in roots drives long-distance transport of NO_3^- from roots to shoots in the *A. thaliana* wild type (Ws) and mutant (*clca-2*).

Culture conditions and plant materials are as described in the Materials and Methods. Differences of NO_3^- flux within the vacuoles in root tissues between Ws and *clca-2* are shown for seedling stage. Mature vacuoles isolated at the seedling stage from roots of hydroponically grown plants (Ws and *clca-2*) were used for measuring NO_3^- flux using the method described in Materials and Methods.

Panel **(A)** values are mean rates of NO_3^- flux during 160 s. The NO_3^- distribution between the vacuole and protoplast is shown at seedling stage **(B)**. Protoplasts and vacuoles isolated from root tissues of hydroponically-grown plants (Ws and *clca-2*) were used to measure NO_3^- concentrations as described in Materials and Methods.

NO_3^- accumulation in the cytosolic shown at seedling stage **(C)**.

P-V total NO_3^- in the cytosol was calculated following as: total NO_3^- in protoplasts – total NO_3^- inside vacuoles. Relative expression of *AtNRT1.5* **(D)** and *AtNRT1.8* **(E)** are shown for root tissues of Ws and *clca-2* at seedling stage. Expression values are relative to that of the actin gene assessed by quantitative RT-PCR as described in Materials and Methods; a value of 1.0 is equivalent to levels of expression of the *Atactin2* gene. Differences of NO_3^- concentration are shown in the xylem sap **(F)**, $[^{15}N]$ S:R ratio **(G)** and $[NO_3^-]$ S:R ratio **(H)** between Ws and *clca-2*. Four weeks old *Arabidopsis* plants were chosen for the assay of the above parameters. Treatments and measurement methods are defined in the Materials and Methods. Wild type *A. thaliana* (Ws), *AtCLCa* mutants (*clca-2*) are described in Materials and Methods. Different letters at the top of the histogram bars denote significant differences (P<0.05). Vertical bars indicate SD (n=6).

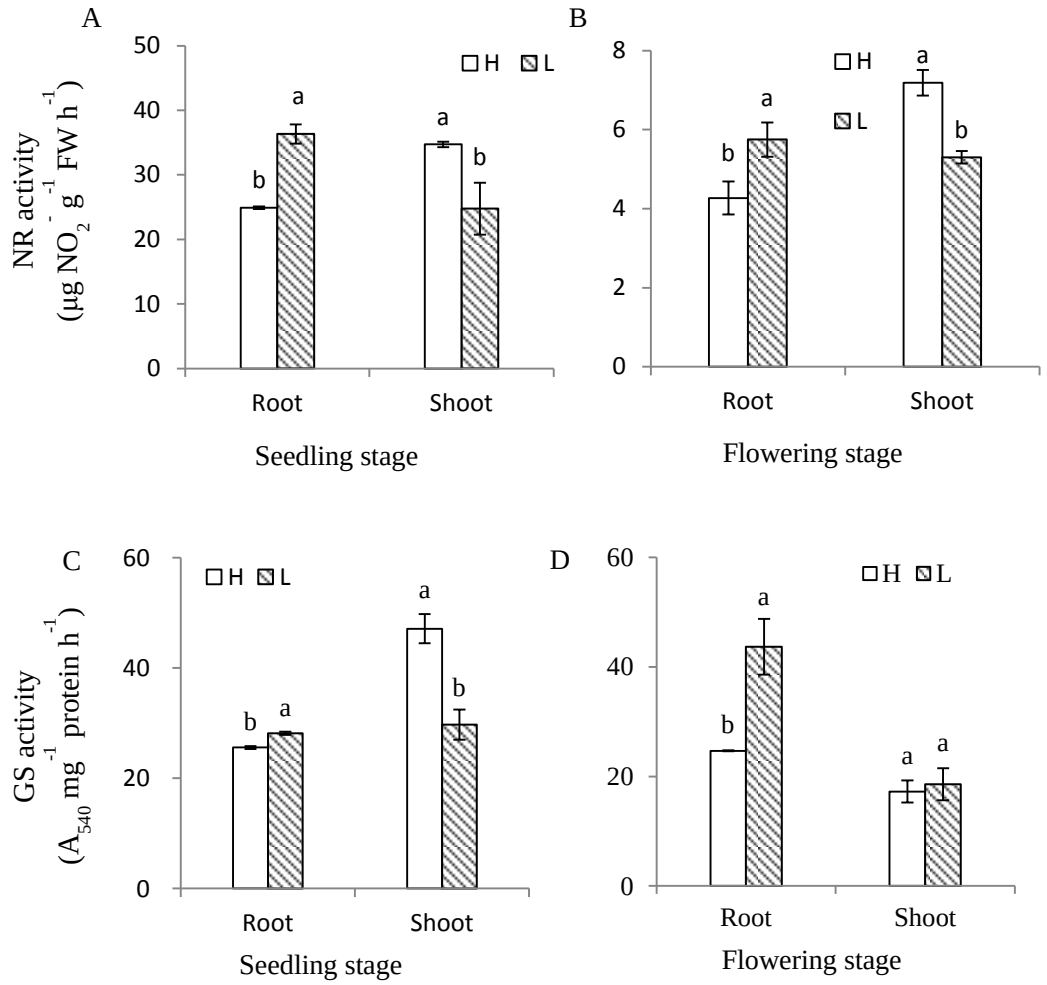

Supplemental Figure 7. Differences of NR and GS activities between the two *B. napus* (H and L genotypes) at seedling and flowering stages.
NR activity in root and shoot tissues of the two *B. napus* genotypes (H and L genotypes) at the seedling **(A)** and flowering stages **(B)**. GS activity in the root and shoot tissues of the two *B. napus* genotypes (H and L genotypes) at seedling **(C)** and flowering stage **(D)**. Vertical bars indicate SD (n=3), different letters at the top of the histogram bars denote significant differences at P <0.05.

A

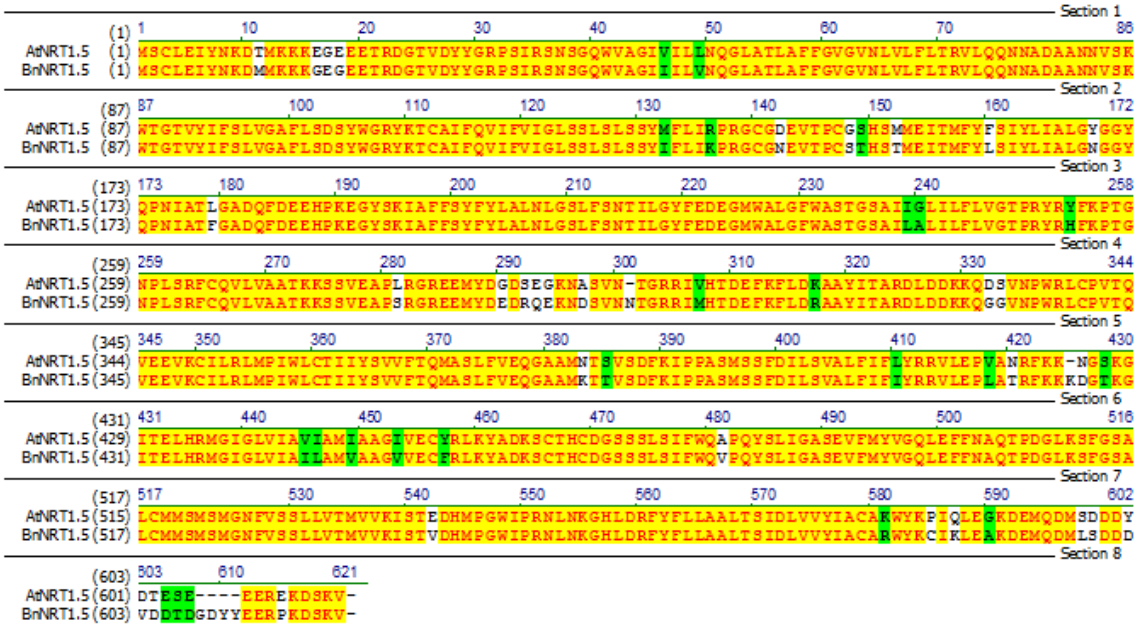

B

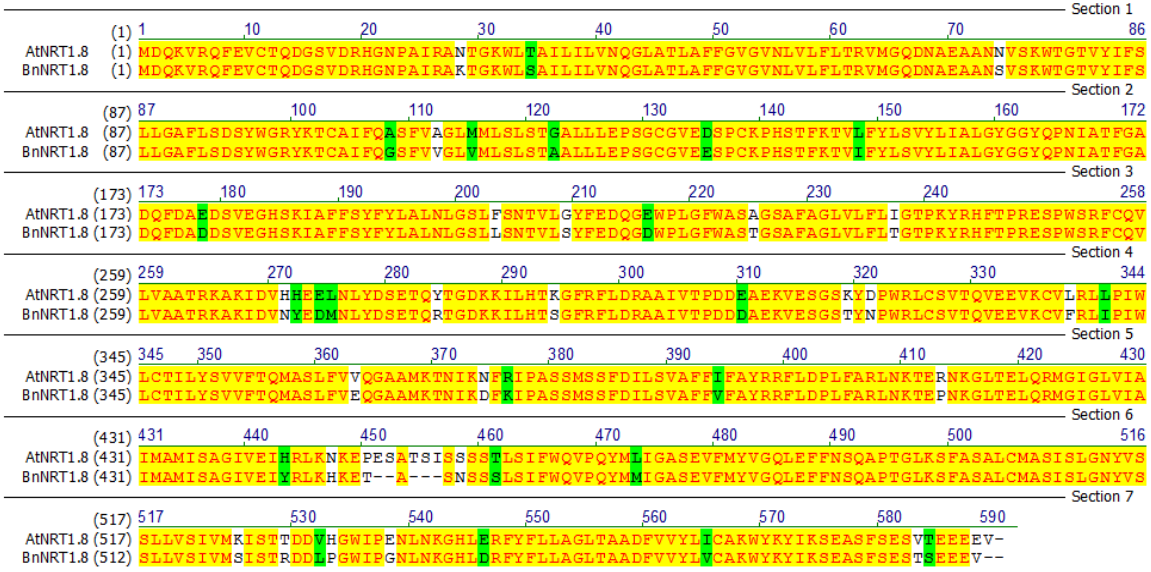

Supplemental Figure 8. Amino acid sequences of *BnNRT1.5* and *BnNRT1.8*. The full nucleotide sequence of *BnNRT1.5* and *BnNRT1.8* obtained from the PCR amplification and the primer design used for PCR amplification of *BnNRT1.5* was based on the nucleotide sequence of *AtNRT1.5* in the *A. thaliana* and GenBank accession EV220114.1; and that of *BnNRT1.8* was based on GenBank accession EV116423.1. Primer sequences for *BnNRT1.5* (*NRT1.5*-F1:tgtatgatgaagatagacaag, *NRT1.5*-R1:gaatcagtttgctgttacatcac; *NRT1.5*-F2:atgtcttgcctagagattta, *NRT1.5*-R2:tgtcatcaagatctcttgctg). The primer sequences for *BnNRT1.8* (*NRT1.8*-F1:gatgactctgttgaaggaca, *NRT1.8*-R1:tatatcacagaacaagctcagct; *NRT1.8*-F2: atggatcaaaaagttagaca, *NRT1.8*-R2:aaagcagagcctgtagacg).
The coding region of *BnNRT1.5* was 1863 bp long, and encodes 620 amino acids, the similarity of nucleotide and amino acids sequences between *AtNRT1.5* and *BnNRT1.5* were 89.4% and 90.0%, respectively **(A)**.
The coding region of *BnNRT1.8* was 1752 bp long and encodes 583 amino acids. Similarities between nucleotide sequences and amino acid sequences of *AtNRT1.5* and *BnNRT1.5* were 88.1% and 90.8%, respectively **(B).**

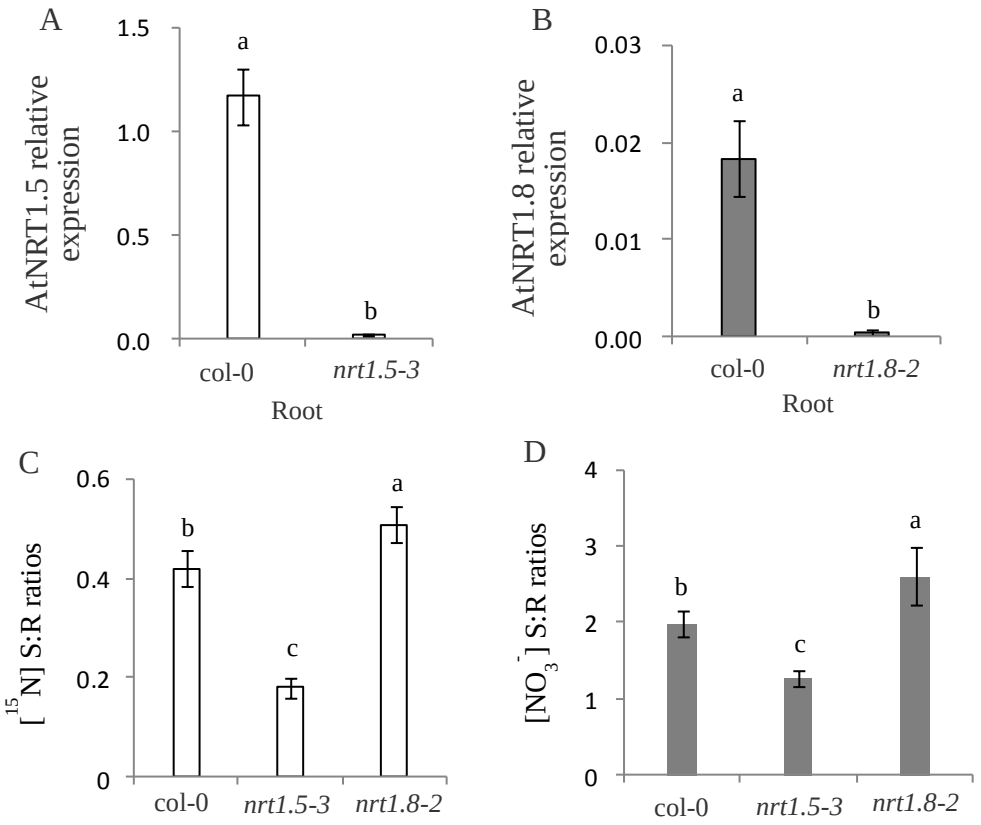

Supplemental Figure 9. Functions of *AtNRT1.5* and *AtNRT1.8* genes in root tissues of *A. thaliana* in controlling NO_3^- long-distance transport from roots to shoots.

Treatment and measurement methods, culture conditions and plant materials are described in the Materials and Methods. Expression of *AtNRT1.5* and *AtNRT1.8* are described in Materials and Methods and in Figure S5. Abbreviations of the mutant and wild-type names are described in the legends to Figures S1. Relative expression of *AtNRT1.5* in root tissues of col-0 and *nrt1.5-3* at the seedling stage **(A)**. Relative expression of *AtNRT1.8* in root tissues of col-0 and *nrt1.8-2* at the seedling **(B)**. Differences are shown for [^{15}N] S:R ratio **(C)** and [NO_3^-] S:R ratio **(D)** between col-0, *nrt1.5-3* and *nrt1.8-2*. Different letters at the top of the histogram bars denote significant differences (P<0.05). Vertical bars indicate SD (n=3).

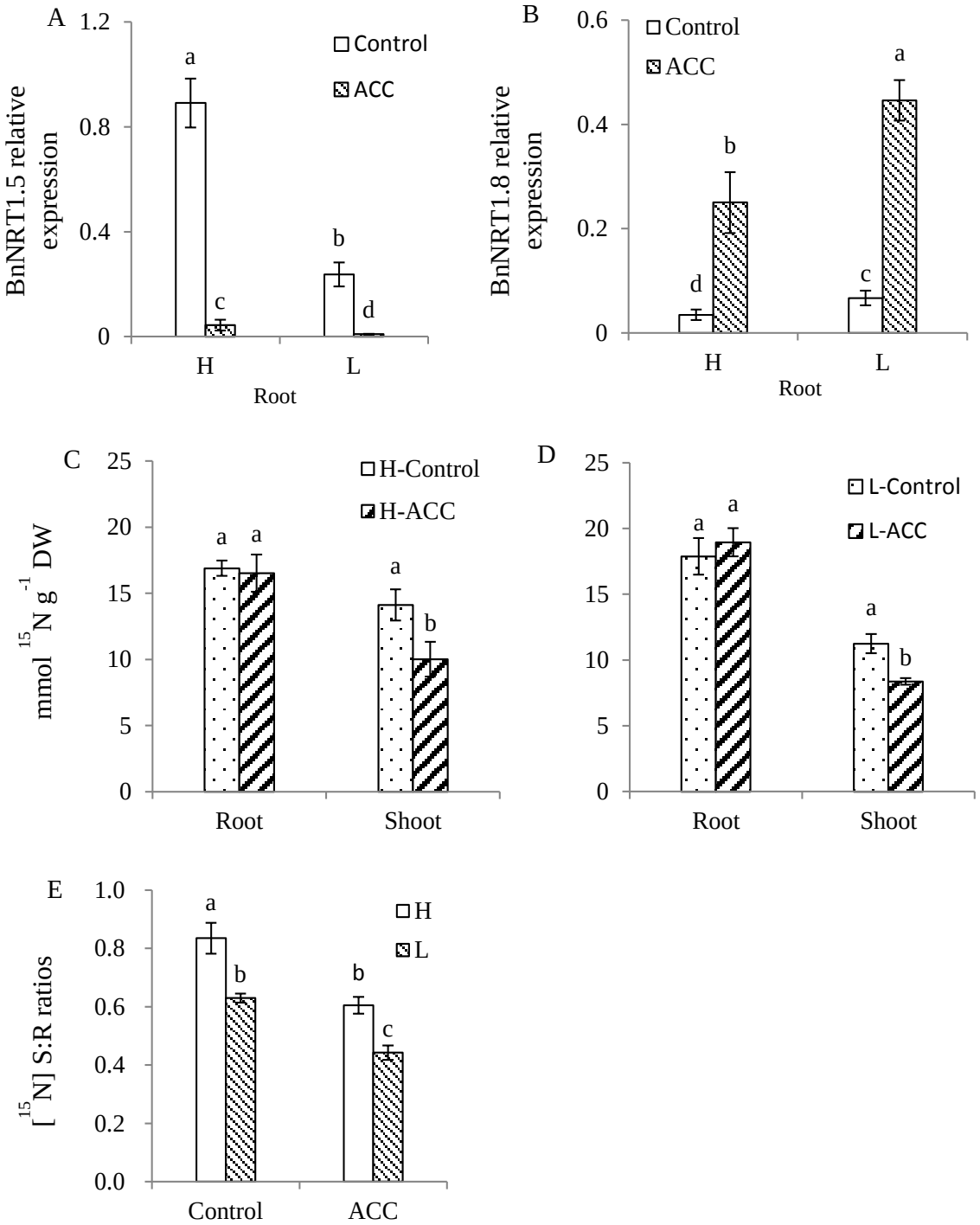

Supplemental Figure 10. *B. napus* *BnNRT1.5* and *BnNRT1.8* genes in root tissues were coordinately modulated to facilitate NO_3^- long distance transport from roots to shoots. *BnNRT1.5*expression in root tissues was down-regulated by ACC treatment at seedling stage **(A)**. *BnNRT1.8* expression in root tissues was up-regulated by ACC at seedling stage **(B)**. Expression of *BnNRT1.5* and *BnNRT1.8* relative to that of the actin gene was assessed by quantitative RT-PCR as described in Materials and Methods; a value of 1.0 is equivalent to levels of expression of the *Bnactin* gene. Effects of ACC on the distribution of ^{15}N between the root and shoot tissues are shown for the H genotype **(C)** and L genotype **(D)** and its effects on [^{15}N]S:R ratios between the H and L genotypes of *B. napus* are shown in **(E)**. Vertical bars indicate SD (n=3), different letters at the top of the histogram bars denote significantly differences at $P<0.05$ level.

Supplemental Table 1. Differences in stomatal conductance and transpiration rate between the two *B. napus* genotypes

Genotypes	Seedling stage		Flowering stage	
	Stomatal conductance[a] (mol H_2O m^{-2} s^{-1})	Transpiration rate (mmol H_2O m^{-2} s^{-1})	Stomatal conductance (mol H_2O m^{-2} s^{-1})	Transpiration rate (mmol H_2O m^{-2} s^{-1})
H	0.33±0.03a	5.26±0.35a	0.24±0.03a	2.48±0.25a
L	0.26±0.01b	4.89±0.13b	0.16±0.02b	1.76±0.14b

[a]Measurements of stomatal conductance and transpiration rates were conducted at 1000 h using a LI-6400 Portable Photosynthesis System. Measurements were made on the 4th leaf from the bottom at seedling stage and the 12th leaf from the bottom at flowering. Different letters denote significant difference between the two genotypes at P<0.05 level, SD (n=6).

Supplemental Table 2. Sequences of primer[a] used for qRT-PCR

Gene information	Forward primer	Reverse primer
BnActin (AF111812)	GGTCGGGACCTCACTGATTC	CAACGGAATCTCTCAGCTCC
BnNRT1.5 (EV220114)	CAATCTACTTGATCGCATTG	CCTGTAGGCTTGAAGTTTCG
BnNRT1.8 (EV116423)	GGCAAATGGCTCAGTGCTAT	GCAACCACTTGGTTCAAGTA
AtActin2(AT3g18780)	TCGGTGGTTCCATTCTTGCTTC	TGGACCTGCCTCATCATACTCG
AtNRT1.5 (At1g32450)	TGGAGCGTTTCTCAGCGATT	TCCATCATGGAATGTGAACCAC
AtNRT1.8(At4g21680)	TCTTCATCTTCGCATACAGGCGGT	GCCATTATCGCAATCACAAGCCCA

[a]Primer sequences optimized in our laboratory using published data are described further in Materials and Methods.